Annu. Rev. Phys. Chem. 1997. 48:243–70

AB INITIO DYNAMICS OF SURFACE CHEMISTRY

Michelle R. Radeke and Emily A. Carter
Department of Chemistry and Biochemistry, Box 951569, University of California, Los Angeles, California 90095-1569; e-mail: eac@chem.ucla.edu

KEY WORDS: interfaces, kinetics, theory, simulation

ABSTRACT

We review the young field of ab initio molecular dynamics applied to molecule-surface reactions. The techniques of ab initio molecular dynamics include methods that use an analytic potential energy function fit to ab initio data and those that are fully ab initio. In this review, we focus on the insights provided by ab initio–based molecular dynamics that are currently unavailable from experimental studies and discuss current techniques and limitations. As an example of how different aspects of a problem can be tackled with state-of-the-art theoretical tools, we consider the well-studied case of H_2 desorption and adsorption from the Si(100)-2 $\times$ 1 surface.

Introduction

In the past ten years, ab initio molecular dynamics (AIMD), or simulations of the dynamic and kinetic behavior of systems with some input from ab initio calculations, have begun to play an important role in surface chemistry (1). AIMD complements experimental observations by predicting reaction pathways, distribution of energy in products, how the distribution of energy and molecular orientation affect reactivity with the surface, and the influence of surface features (steps, defects) on dynamics and reactivity. In this review, we look at how these techniques fare at describing reactions in which a molecule interacting with a surface undergoes a chemical change involving bond breaking or bond formation.

The holy grail of AIMD is to be able to perform fully ab initio molecular dynamics simulations (FAIMD) of large, realistic systems over long time scales,

0066-426X/97/1001-0243$08.00

including full electron correlation. We are a long way from being able to perform such calculations. While the search for more efficient methods goes on and continuing breakthroughs in computer architecture permit increasingly more complex simulations, what we now have available in AIMD are several methods that allow us to investigate different aspects of a problem. Furthermore, what is considered state of the art for AIMD of surface chemistry depends on the system and the goal of the calculation.

We can divide AIMD techniques into two broad categories: (*a*) methods that require an explicit, analytic potential that has been fit to ab initio data and (*b*) those that determine the relevant potential energy surface (PES) features through ab initio calculations, which are performed as needed during the simulation (on the fly). In the former category, we have classical molecular dynamics (MD), quantum dynamics (QD), and Monte Carlo variational transition state theory (MC-VTST). In the latter group we have FAIMD. Outside of both categories we have ab initio–derived kinetic Monte Carlo (KMC) simulations, which can use rate constants determined from a variety of methods. Straddling the categories is nonvariational TST, which requires a Hessian (energy second-derivative matrix) evaluation of the system (which can be determined from either an analytic potential or from ab initio calculations).

The main disadvantage of calculations that fall into the first category is that the results are limited by the quality and functional form of the analytic potential function that is used. The ability to perform the necessary ab initio calculations also limits the type of systems that can be investigated. The analytic potential, nevertheless, makes it easy to calculate molecule-surface interactions so that larger systems and/or longer time scales can be simulated than if the ab initio calculations were performed on the fly during the dynamics run. Because the quality and form of the potential dictate the results from these types of simulations, the most accurate of these calculations are done with realistic analytic potentials fit to ab initio data.

QD simulations have an obvious advantage over MD simulations in that in an MD simulation, Newton's equations of motion determine the evolution of the system, whereas in a QD simulation, the time-dependent Schrödinger equation is propagated, introducing quantum effects such as tunneling and zero-point energy (ZPE) (2a,b). These effects are particularly important for light molecules interacting with surfaces, for instance H_2. On the other hand, as a result of the exponential growth of the number of degrees of freedom with the number of particles in a quantum system, only a few degrees of freedom in the problem can be treated using a full quantum description. Because including surface motion can rapidly introduce many new dimensions into the calculation, these calculations tend to be limited to events that occur on a time scale of hundreds of femtoseconds or less, during which the substrate may be considered

frozen. Currently, the highest number of dimensions that have been included in a quantum dynamical simulation of surface chemistry is six (3a–c). Classical simulations, by contrast, can include the full dimensionality of the surface and molecule, with current practical computational limitations of these simulations being on the order of nanoseconds or less, depending on the complexity of the PES and the number of atoms included (4).

Recently, KMC techniques have been developed to allow a more realistic time scale in dynamical models. KMC correlates real time to Monte Carlo steps through establishing a hierarchy of independent events in the simulation, determined by the relative rate constants of the processes (5). Thus, the input to KMC calculations are the rate constants of the various processes being simulated. In principle these rate constants can be guessed, but for more quantitative simulations ab initio–determined rate constants should be used.

TST methods provide the means of obtaining chemical reaction rate constants. One such procedure, MC-VTST (6a–8), requires an explicit analytic PES. This technique allows an upper bound for a rate constant for an elementary reaction step to be evaluated, provided that the PES is sufficiently accurate. However, dynamical corrections are needed to correct for the neglect of barrier recrossings and correlated sequential steps (e.g. multiple hops in diffusion) in this model.

On the other hand, a nonvariational, simple TST (STST) can be used with either an analytic potential function or ab initio calculations to determine the Hessian from which the necessary frequencies are derived. This method provides a rough estimate of the rate constant by using the harmonic approximation to evaluate the preexponential, A, of the rate constant $k = Ae(^{-Ea/k_BT})$ as $A = (\Pi^{3N-6}\nu_{\min})/(\Pi^{3N-7}\nu_{\text{sad}})$. In this equation, A is the ratio of the product of the nonzero vibrational frequencies at the minimum (the reactant) to the product of the real, nonzero vibrational frequencies at the TS (thus the imaginary frequency at the TS is excluded) (9).

For post–Hartree-Fock (HF) wavefunction-based energy and gradient calculations, surfaces can be modeled using only embedded and/or finite clusters (not an infinite surface). Since metal surfaces are generally not described well by a cluster, owing to the delocalized, long-range nature of the electronic wavefunction, the applicability of this method is limited to surface reactions on covalently bound solids such as semiconductors, where it has been used successfully to describe localized bonding (10a–15). For density functional theory (DFT) (16a,b), a periodic slab can be used as an alternative approximation to an infinite surface. However, DFT methods have not yet been tested for rate constant evaluations. Also, DFT has not been well tested for evaluating the activation energies that appear in the exponential of the rate constant expression given above. The main disadvantages of nonvariational TST are the errors

incurred by the harmonic approximation and the fact that the computed rate constant cannot serve as an upper bound.

The most promising methods for viewing realistic dynamics are FAIMD simulations in which no explicit PES is required, because the forces on the nuclei are calculated directly from the quantum mechanics at each time step. Since the movement of the nuclei does not depend on an analytic function for the energy, as in traditional MD, FAIMD calculations are not intrinsically biased toward certain outcomes by the form of the potential. Two advantages of FAIMD calculations are not having an analytic potential form prejudice the dynamics and not needing to specify an analytic potential; these allow many different systems to be simulated without the time-consuming process of deriving and fitting potential energy functions. These methods, however, are currently limited in their scope because of their computationally intensive nature (multiple evaluations of quantum mechanical energies and gradients are needed to predict dynamics), and although improvements in computer architecture and AIMD methods have helped somewhat, simulations of large molecule-surface systems are not yet practical.

The first FAIMD method formulated was the method of Car & Parrinello (CPAIMD) (17), which used Kohn-Sham DFT (18) to describe the electrons. In this technique, instead of diagonalizing the Kohn-Sham equations at each MD time step, the Kohn-Sham orbitals are given fictitious masses and propagated classically, thus saving computational time. However, the alternative method, explicitly evaluating the Kohn-Sham orbitals at each time step, is computationally comparable to CPAIMD for DFT with plane-wave basis sets, since longer time steps may be used (19a,b, 20). Because the evolution of the system is guaranteed to remain on the Born-Oppenheimer surface when the density is optimized at each time step, this version of FAIMD is termed Born-Oppenheimer AIMD (BOAIMD).

FAIMD techniques are most commonly implemented using plane-wave–based DFT techniques to evaluate the energy and gradient, as cheap (to calculate) Hellman-Feynman forces are nearly exact in this case, which makes FAIMD computationally tractable. A watershed event for simulating more realistic systems using DFT was the invention of pseudopotentials, which dramatically decreased the number of plane waves needed in DFT calculations by eliminating the need to include the atomic core electrons (20, 21a,b). A DFT-based procedure has the advantage of being less time consuming [$O(N^3)$ at worst] than wavefunction-based quantum mechanics methods, allowing larger systems to be considered. Thus in plane-wave–based DFT, periodic slabs arise naturally and can be used to represent a surface, rather than the embedded clusters that wavefunction-based quantum methods are restricted to as a result of their prohibitive scaling [$O(N^4)$ or worse].

DFT-based techniques do have serious disadvantages, however. Among other issues is a lack of systematic inclusion of full electron correlation, which compromises descriptions of surface bonding. There is also arbitrariness in the choice of the pseudopotentials—small changes in the pseudopotential can lead to large changes in energy differences and other properties. Accuracy issues related to DFT are discussed below.

Wavefunction-based AIMD (WBAIMD) methods—for example HF (22, 23), generalized valence bond (GVB) (24, 25), and complete-active space self-consistent field (CASSCF) (26, 27)—are more time consuming than DFT-based AIMD, for several reasons. The atom-centered Gaussian basis functions required by wavefunction-based methods mean that the integrals over the basis functions change as the atomic positions change and thus they must be recalculated at each time step. Also, the Hellman-Feynman forces, which are good approximations for DFT-based AIMD, work poorly in WBAIMD, necessitating full gradient calculations. In spite of this, these methods are worth looking at because they bring with them several important advantages. In the GVB and CASSCF procedures, electron correlation is explicitly included in the configuration interaction (CI) expansion, yielding better bonding descriptions and proper bond dissociation. Nevertheless, the results are only qualitatively correct. For quantitative accuracy, multireference single and double excitation configuration interaction (MRSDCI) (28) calculations are needed. And, as noted above, these methods are limited to small systems for which a cluster description of the surface is suitable, for instance, covalently bonded solids but not metals. As was found for DFT-based AIMD, wavefunction-based BOAIMD with a sufficiently converged wavefunction, is more numerically stable than CPAIMD, allowing the use of longer time steps, which increases its efficiency (29, 30).[1]

To date, most AIMD calculations of surface chemistry have focused on the dissociative adsorption (primarily on metal surfaces) of H_2 and other diatomics. Recently, there have been more calculations on larger molecules and clusters, mainly on metals, metal oxides, silicon, and diamond. In this review we attempt to cover as much of this area as possible. We begin by reviewing dynamics that use an ab initio–derived analytic potential function in classical MD and

[1]For WBAIMD there is no advantage to using the CP technique over the BO method, as the dominant part of the calculation is the determination of full analytic forces, not the calculation of the wavefunction. Recently, da Silva et al (30) revisited wavefunction-based CP MD, since a constraint term in the equations of motion for the nuclei had been inadvertantly omitted in the work of Gibson et al (29). They found that when these constraints are correctly accounted for, CPAIMD is still less efficient than BOAIMD, in fact more so than was stated in Reference 29, because of the iterations involved in the constraint algorithm. Thus the conclusions of Gibson et al (29) do not change, namely that BOAIMD is still more efficient for atom-centered bases.

QD. Following this, we discuss the calculation of rate constants using ab initio calculations. FAIMD simulations are also discussed. To illustrate what can be learned by applying the different AIMD techniques to aspects of a scientific problem, we then consider the case of H_2 adsorption and desorption on Si(100). As mentioned above, accuracy issues related to AIMD are then discussed. We conclude with an assessment of needed improvements to AIMD.

We have meant this review to focus on AIMD of molecular-surface reactions and to be as inclusive as possible without covering subjects that have been previously reviewed. This excludes any MD performed using a potential energy surface which is not fit to ab initio gas-surface interactions (thus studies using analytic potentials fit to gas-phase ab initio calculations are not included).

Classical Molecular Dynamics with an Ab Initio–Derived Analytic Potential

The first example of applying AIMD to molecule-surface interactions in a classical MD simulation using a potential for which all gas-surface interactions were fitted to ab initio data is the study by Carter and coworkers (31a,b) of fluorine reactions with the Si(100)-2 × 1 surface. Prior to this work, only an empirical potential created by Stillinger & Weber (SW) was available, with the homoatomic parameters (32) fit to bulk Si and F_2 gas data and the heteratomic parameters (33) describing the Si-F interactions fit to gas-phase SiF_x and Si_2F_6 properties. Using their potential, SW performed simulations (32, 33) that resulted in two physically unreasonable conclusions: (*a*) Etching of Si occurred only when the surface was allowed to melt, at odds with the observed spontaneous etching that occurs at room temperature, and (*b*) F_2 molecules had a nonzero scattering probability on clean Si(100), in disagreement with the molecular beam experiments of Ceyer and coworkers (34). Also using the SW potential, Schoolcraft & Garrison (35) performed calculations of high-energy (3 eV) F atoms impinging on the Si(100) surface that predicted spontaneous etching under these conditions.

To give a more accurate representation of F_2 interacting with the Si(100) surface than provided by the gas-phase data used in the SW potential, Wu & Carter performed highly correlated ab initio calculations of fluorine approaching and bonding with the Si(100) surface (represented as an embedded cluster) (36a,b). Comparing the original SW potential to these ab initio calculations, Weakliem, Wu, and Carter (WWC) determined that the overall shape of the SW potential was a reasonable fit to the ab initio calculations but that the well depth of the SW potential for Si-F bonding was much too shallow (by as much as 4 eV) and nonbonding terms were too repulsive (31a,b). Thus the SW potential was found to be too repulsive to allow the isothermal formation of the fluorosilyl layer necessary for etching to occur, which explained why previous

isothermal simulations did not yield even initial formation of the fluorosilyl layer by thermal fluorine.

Since the analytic form of the SW potential seemed adequate to describe the Si-F interactions if the well depths were adjusted to fit the ab initio CI predictions, WWC refit the SW Si-F potential to these data (31a,b). Using the WWC potential in MD simulations, Carter and coworkers were able to see the initial buildup of the fluorosilyl layer. However, the time scale of MD simulations for this system is on the order of hundreds of picoseconds, while in reality, deposition of a fluorine multilayer and etching occurs on the order of seconds. Thus the MD simulations necessarily use a much faster deposition rate of fluorine than is realistically possible in order to observe rare event processes such as formation of SiF_2 and SiF_3. The limitation on time in MD simulations meant that Carter and coworkers (31a,b) could observe only the initial buildup of a disordered fluorosilyl layer and not true etching, which occurs on much longer time scales. This time scale problem could be dealt with in a KMC simulation; however, in order to do this, more ab initio calculations would be necessary in order to include various subsurface Si-F interactions, and a new potential would have to be fit, since the WWC potential is fit only to Si-F surface interactions.

Despite the time scale limitations, one key prediction of this 1992 study was later borne out by X-ray photoelectron spectroscopy experiments (37): The tremendous exothermicity of the reaction of fluorine with silicon leads to local-heating–induced disorder of the Si lattice in near surface layers (see Figure 1). This disorder opens up more reaction sites (so-called dangling bonds) to allow further reaction with fluorine in an autocatalytic manner. The concept of lattice disorder being critical for etching was introduced in this study and exploited in later work in which Carter & Carter (38, 39) showed how an ordered fluorine overlayer could be used as a self-mask to inhibit further reaction.

Other interesting information about the nature of fluorine reactions with the Si(100) surface can be learned from the MD simulations. By computing enough trajectories of a single fluorine molecule impinging on the Si(100) surface to get statistical results, Carter and coworkers (39, 40a–c) were able to perform a detailed analysis of the factors that enhanced fluorine reactivity, providing insight into how internal energy distribution, molecular orientation, surface coverage, steps, and defects affect dissociation probability. One key finding from these studies was that translational activation is highly effective at increasing the reaction probability; indeed, the reaction probability can be tuned as a function of the fluorine incident kinetic energy. Another startling prediction was that low-energy fluorine molecules preferentially deposit one, not two, fluorine atoms on silicon surfaces (39, 40a–c). Ceyer and coworkers' molecular beam scattering experiments (34) also suggested that this was occurring, and Kummel and

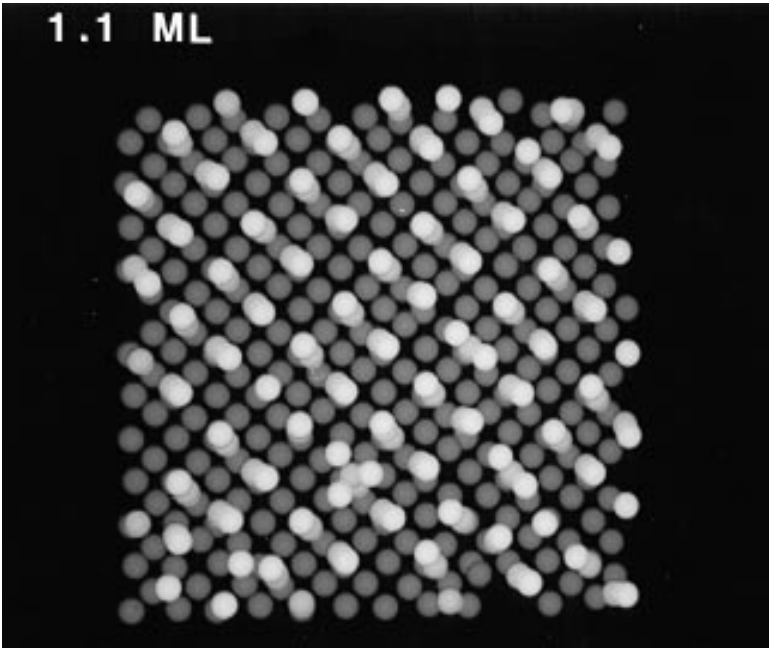

Figure 1 Top view of a Si(100) surface that has been exposed to fluorine gas in an ab initio–derived MD simulation. The white spheres are F atoms, the top layer of Si is depicted as light gray spheres, while the rest (dark gray spheres) are subsurface Si. Note the presence of SiF, SiF_2, and SiF_3 groups on the surface, even at the low coverage of 1.1 monolayers, and the initial onset of disorder, as illustrated by the disruption of the (light gray) Si dimer rows. (Adapted from Reference 31a.) [A color version of this figure is available on the World Wide Web in the Supplementary Materials Section of the main Annual Reviews Inc. site (http://www.annurev.org).]

coworkers later directly confirmed this prediction by using scanning tunneling microscopy (41). The reaction also was found to produce highly inelastically scattered F and F_2 by-products that are rendered nonreactive. Carter & Carter (39) suggested that the reactivity of translationally excited F_2 combined with the subsequent nonreactivity of the gas phase by-products might allow for more highly anisotropic etching. Thus results from AIMD were shown to lead to new design principles for surface etching.

Garrison and coworkers (42) performed an informative comparison of the SW and WWC potentials for F_2 reacting with Si(100). They found that neither parameterization predicts adequate levels of F_2 dissociative chemisorption when compared with experiment, but the SW parameterization predicts significantly less dissociative chemisorption than the WWC parameterization. Their study

and the above work of Carter and coworkers suggest that while the WWC potential is an improvement over the SW potential, both are still too repulsive and that additional high-level ab initio calculations are needed to better describe F-Si(100) interactions (38).

This tactic of using ab initio data to improve analytic potentials and then performing classical dynamics has also been applied to the interaction of H_2 with metal surfaces. Classical dynamics are expected to be a good approximation for F_2-Si(100), since the heavy fluorine atoms are not anticipated to exhibit quantum effects when interacting with the Si surface. In the case of molecular hydrogen chemisorption, however, quantum effects could be substantial, except at elevated temperatures. This is discussed more in the following section on QD. Nevertheless, classical dynamical simulations have yielded qualitative agreement with experiment.

The first of these is a study by Kara & DePristo (43), who used generalized Langevin equation (GLE) classical MD to compare site selectivity and molecular orientation for two systems, H_2-Ni(100) and N_2-W(110). The H_2-Ni(100) study is an example of a PES fit with ab initio data: Kara & DePristo (43) refit the two-body (H-Ni) parameters of the London-Eyring-Polanyi-Sato (LEPS) PES of Lee & DePristo (44) to ab initio CI data of H-Ni(100) interactions (45a,b) [They were unsuccessful in fitting the four-body LEPS (H_2-Ni) parameters to available ab initio CI data and instead adjusted the parameters pertaining to H_2 dissociation to fit experimental measurements (46).] For the reaction of N_2 on W(110), however, they used an empirical potential. Interestingly, they found that H_2 adsorption on Ni(100) is very site specific, despite a high adsorption probability, whereas the adsorption of N_2 on W(110) was not site selective at all, despite a low sticking probability. Kara & DePristo (43) reasoned that because incoming H_2 molecules are focused into adsorption sites by the PES, the sticking probability remains high despite strong, thermodynamically driven adsorption site preferences. For the larger nitrogen molecule, however, molecular orientation was much more important for the occurrence of dissociative adsorption than the location of the adsorption site on the W(110) lattice, since all adsites were thermodynamically favorable on W and parallel orientations of the N_2 were strongly preferred dissociation precursors. Kara & DePristo's prediction of a low sticking probability for dissociative adsorption of N_2 on W(110), even at high incident energies, coincides with experimental results. Thus they suggested that strong reaction dependence on molecular orientation generally will lead to subunity sticking probabilities. This has certainly been borne out in subsequent experimental studies, such as the work of Michelsen et al for H_2 on Cu surfaces (47). Another interesting prediction this study makes is that high symmetry sites are not the dominant dissociation sites. These predictions suggest that ab initio data used to fit analytic PESs must sample a multitude

of surface adsorption sites and molecular orientations in order to sufficiently describe molecule-surface interactions.

In the next section, we discuss Jackson & Metiu's QD investigation of H_2 dissociation on Ni(100) (48). This work shows some of the limitations of classical dynamics for this system, but a comparison between the classical dynamics work of Kara & DePristo (43) discussed above and the QD study of Jackson & Metiu (48) is difficult to make because the classical simulation includes all degrees of freedom of those atoms explicitly included, while the QD calculation is a restricted two-dimensional model. Furthermore, the classical study utilized a PES that favors center-site dissociation, while the PES used in the QD treatment predicts a reaction at the on-top site (over an atom). Since six-dimensional calculations are now possible, a comparison of the new, higher-dimensional QD with classical dynamics predictions for this system (using the same PES, of course) would ascertain under which conditions classical dynamics is an appropriate model. However, even a six-dimensional QD calculation would not be sufficient to describe all possible trajectories of H_2 impinging on a nonrigid surface.

Recently, GLE quasiclassical MD of H_2 reacting with the Ni(111) surface have been carried out by Tantardini and coworkers using two ab initio–derived analytic potentials of different quality (49, 50). Both studies used a LEPS potential function to describe the molecule-substrate interactions. In both reports, the potential was built from ab initio (limited CI) binding energy curves using embedded cluster models of H-Ni(111) (51a,b, 52), but the PES in Reference 50 utilized a larger cluster and hence was deemed to be of higher quality. With each of these potentials, Tantardini and coworkers examined the dependence of the H_2 dissociative adsorption probability on the incoming H_2 molecules' internal and translational energies, incident molecular beam angle, surface temperature, and surface corrugation. The accuracy of their results was benchmarked using experimental data pertaining to the increase in sticking probability with increased translational energy of the H_2 molecular beam. In the first work, Bourcet & Tantardini (49) used the rigid surface approximation that allows no transfer of energy between the molecule and substrate and achieved some qualitative agreement with experiment. In the later work, Forni & Tantardini (50) used their improved potential in simulations using both the rigid and nonrigid surface approximations. (Note that their approximation for the nonrigid metal surface was a set of coupled harmonic oscillators.) Simulations using the new, improved potential with the rigid surface yielded a dissociative adsorption probability curve that was not even in qualitative agreement with experiment. (Their reported curve was S-shaped and increased rapidly with the collision energy rather than smoothly increasing as demonstrated in experiments.) However, when the rigid surface approximation was removed, their calculations

were in good agreement with experiment. Thus, the agreement of theory with experiment in the earlier work using a rigid surface and a less accurate PES was fortuitous. Their work (49, 50) illustrates that the same underlying analytic form of a potential can give wildly different results that depend on the type and quality of data it is fit to, which underlines the importance of accurate ab initio data. Furthermore, their work highlights the inadequacies of the rigid surface approximation.

Another point of concern is that a completely contradictory qualitative conclusion was reached in these two sets of studies of H_2 incident on Ni surfaces at nearly the same incident energies, albeit on two different crystal faces of Ni: Kara & de Pristo (43) concluded that H_2 orientation had little or no effect on the sticking probability, while Forni & Tantardini (50) concluded just the opposite for low collision energies. This leads one to suppose that highly approximate treatments of the surface electronic structure (as in these two studies) will lead to highly variable predictions not only in a quantitative but also in a qualitative sense and again points out the need for an accurate ab initio description of the surface and the surface-adsorbate interaction in order for predicted dynamics, energetics, and kinetics to be reliable.

Forni & Tantardini (50) discussed how properties of these two potentials combined with molecule-substrate energy transfer influence the sticking probability. In particular, they found that the adsorption probability was greatly reduced by surface motion. They also found that vibrational excitation was less effective than translational excitation in enhancing dissociation; Carter and coworkers found this same result for F_2 reacting with Si(100) (39, 40a–c). The different nature of these systems' interactions suggests that in general, translational excitation is more effectively transferred into the dissociative reaction coordinate than is vibrational excitation. This is most likely to be the case where the barrier to dissociation is early, i.e. in the entrance channel.

As far as we know, no classical MD studies have used potentials for H_2 interacting with metal surfaces where the H_2-metal interactions (rather than just H atom and metal interactions) have been fit to ab initio data. [This is also a limitation of the F_2-Si(100) studies, where the potential was fit to F atom–surface Si interactions (31a,b, 36a,b).] Comparisons of the accuracy of this type of PES to one fit with only ab initio H atom–metal interactions is still necessary, as is comparison of the QD and classical MD methods. And, as mentioned above, another common weakness shared by the calculations discussed thus far is that the surface itself is typically described using an empirical potential (e.g. SW for Si) or at best a semiempirical description (e.g. de Pristo's work on Ni). Once the error in these types of calculations is known, then better judgments can be made as to which type of PES and which approximations are appropriate in the balance between computational tractability and accuracy.

Quantum Molecular Dynamics with an Ab Initio–Derived Analytic Potential

QD calculations performed using an ab initio–derived PES have almost exclusively dealt with H_2/D_2 reactions with metal surfaces. An exception is the desorption of H_2 from Si(100) discussed below. Holloway and Holloway & Darling have published several excellent reviews on QD applied to molecules interacting with surfaces, including a discussion of the effects of surface corrugation (53); a review on reactive/nonreactive scattering, from the Lennard-Jones potential model to classical MD to QD (54); and recently an in-depth review of all the major theoretical techniques for describing dissociative adsorption, focusing on diatomics reacting with metal surfaces and H_2 dissociative adsorption (55). Because of the multitude of reviews on this subject, we briefly summarize this topic and keep our focus on how ab initio–derived PESs improve the QD picture.

In general the studies of H_2/D_2 interactions with metal surfaces investigate effects of surface corrugation, the vibrational/rotational dependence of dissociative adsorption, and tunneling effects. We note that in their 1995 review of QD of H_2 dissociation on metal surfaces, Holloway & Darling (53) discussed the insight provided by ab initio calculations that show energetic and geometric corrugation for H_2 interactions on PESs normally considered smooth [e.g. Cu(111) and Mg(0001)] (56, 57a,b).

As mentioned above, Jackson & Metiu performed an early study (48) of the QD of H_2 dissociation on Ni(100) using a LEPS potential fit to ab initio CI data of the transition state and adsorbate regions for H_2 adsorption over the on-top site of the Ni(100) surface (58). Since the barrier is negligible for dissociation at this site, they reasoned that this was a probable place for H_2 sticking on Ni(100) and limited their QD study to a restricted two-dimensional [i.e. R(H-H) and distance to the surface] model of dissociation. They found that H_2 dissociation on this surface is quite nonclassical, with multiple reflections between three possible (low) barriers being the exception rather than the rule, even at fairly high incident energies. They varied the values of barriers to molecular chemisorption, dissociative chemisorption, and H atom surface diffusion. If the barrier to diffusion was even only slightly higher than the barrier to dissociative adsorption, then significant reflection resulted in H atom recombination to reform $H_{2(g)}$ (e.g. if the diffusion barrier height is only 0.15 eV higher than that for dissociation, 99% of the H atoms recombined!). Thus, an insightful concept was born: Dissociation is only achieved if recombination is suppressed by low diffusion barriers so that H atoms may escape to well-separated adsorption sites. They also commented that even 0.05-eV changes in barrier heights drastically affected dissociation rates at typical thermal beam energies, leading us again to

emphasize the essential role played by highly accurate ab initio predictions of barrier heights and PESs in obtaining even qualitatively correct predictions of dynamics and reactivity.

This pioneering two-dimensional QD study by Jackson & Metiu (48) was undertaken ten years ago. Norskøv and coworkers (59) moved beyond two-dimensional QD to include the other four degrees of freedom of the H_2 using the classical hole model. The important result of their work was to compare H_2 dissociation on Al(110) on a PES derived from DFT using the local density approximation (LDA) (60) with one derived from DFT using the generalized gradient approximation (GGA) (61), where these terms affect the form chosen for the exchange-correlation energy functional. They showed that the two different functionals yield starkly different dissociation dynamics. Although one tends to hope that the inclusion of density gradient terms will increase the accuracy of the calculations, their effect tends to vary rather nonsystematically (see section on Accuracy Issues for Ab Initio Calculations).

Kinnersley et al (62) compared QD and MD using a PES derived from DFT-GGA calculations for H_2-Cu(111) on several vibrationally adiabatic two-dimensional PESs (varying a third coordinate parametrically). They found that although quantum and classical dissociation probabilities as a function of initial rotational energy and incident angle are very similar, it is the quantized motion near the saddle point that is responsible for the characteristic structure of dissociation probabilities plotted as a function of incident translational energy. Thus this study showed that in some cases, depending on the behavior in question, classical MD is insufficient.

In the past few years, six-dimensional PESs of H_2 dissociation on metal surfaces have been formulated using DFT calculations (56, 63a,b). The availability of these PESs, improvements in QD algorithms, and rapid gains in computational speed have led to the first six-dimensional QD calculations of H_2 adsorption and desorption (64). A short review by Gross (65) summarized a six-dimensional QD study of H_2-Pd(100) (64) and a recent five-dimensional QD computation of H_2-Cu(111) (66). The major contribution of this series of papers, and of Kay et al (67), who studied H_2 on W(100), was to discuss the concept of steering as an alternative to molecular precursor states in order to explain an increase in sticking with decreasing incident kinetic energy. By comparing a previous two-dimensional H_2-Cu(111) QD calculation (68) to the later five-dimensional calculation (66), Gross concluded that higher dimensionality calculations not only provide quantitative accuracy but also change the qualitative concepts gleaned from the lower-dimensional picture.

In contrast to the high-dimensional calculations from DFT PESs for H_2 on metal surfaces, QD using ab initio–derived potentials of other molecule-substrate systems is very limited. We discuss the example of H_2-Si(100)-2×1

below. Another example is the two-dimensional, two-state model of NH_3 and ND_3 desorption on Cu(111) by Saalfrank et al (69). The purpose of this study was to understand photodesorption of ammonia from this surface. They used ab initio calculations [restricted open-shell HF followed by second-order Møller-Plesset perturbation theory (MP2)] (70, 71) to obtain information about the position and depth of a second minimum for NH_3 adsorption; this region of the PES is not easily accessible to experimentation. They found a second minimum for ammonia adsorbed in the inverted umbrella position and at a greater N-surface distance than the global minimum (ammonia adsorbed with the N atom pointing toward the surface and the H atoms in a plane above). Their ab initio MP2 data agreed with the general shape of the analytic potential they were using and of the global minimum, but predicted a much shallower second minimum than the analytic potential. They found that it was necessary to use the well depths predicted by the empirical analytic potential function rather than from the ab initio MP2 data in order to obtain agreement with experimental data on ammonia photodesorption. They attributed the difference in well depth to the small cluster size (one metal atom) and a too small (double-ζ plus polarization functions) (72) basis set and reasoned that improvements in both would increase the well depth, thus justifying their use of the empirical potential in their calculations. This clearly indicates yet again the importance of accurate and realistic ab initio calculations in defining PESs for dynamical calculations.

Transition State Theory Using Ab Initio Methods

Ab initio calculations of barrier heights for specific reaction pathways are often compared in order to identify the fastest and slowest steps in surface processes. However, this neglects the effect of the preexponential factor in the Arrhenius equation for the overall rate constant. Transition state theory attempts to remedy this situation by providing estimates for the rate constants directly.

NoorBatcha et al (7) were the first to use the MC-VTST method developed for unimolecular gas-phase reactions and atomic desorption (6a–f, 8) on bimolecular recombinative desorption from surfaces. They applied this procedure to H_2 desorbing from unreconstructed Si(111) (represented by 53 atoms in 3 surface layers) by using an analytic PES fit to ab initio HF calculations on small clusters (73) and experimental data (7, 74). The activation energy determined from an Arrhenius plot was in good agreement with the most recent experimental result, but was significantly higher than two earlier experiments. In order for their calculated Arrhenius parameters to yield the same rate constant as experiments, both of their calculated parameters would need to be in good agreement with the experimental values. However, their preexponential factor for desorption was four orders of magnitude lower than the Arrhenius parameter from the experimental work that best agreed with their activation energy. And, although

their preexponential factor was only one order of magnitude higher than the preexponential factors in the previous two experiments, their predicted activation energy for desorption was 0.6 eV higher than the values obtained in those studies. Looking at the rate constant as a whole, rather than at the agreement of the individual parameters with the experimental range for each of those Arrhenius parameters, suggests a lack of quantitative agreement with experiment. The fact that the potential function was fit to HF calculations (instead of ones that include electron correlation) and the use of a surface model with no reconstruction [at low coverages, Si(111) has a 7×7 reconstruction] both may have been responsible for the discrepancies between theory and experiment. To be fair, these calculations were performed more than 10 years ago and were certainly pioneering at the time.

Skokov et al (75) and Musgrave et al (76) used nonvariational TST to identify important steps in diamond growth. In both of these studies, wavefunction-based ab initio energy and Hessian calculations were performed on clusters of C atoms embedded in H atoms to represent the diamond (100) surface. Skokov et al (75) investigated acetylene (C_2H_2) reacting with surface atoms and dimers represented by C_9H_{12} clusters. They used a standard 6-31G** basis set in unrestricted HF (UHF) calculations to determine optimized structures and spin-projected MP2 theory to calculate energy barriers. Vibrational frequencies were evaluated using MOPAC routines. Analysis of several mechanisms for adsorption and desorption led to their predictions that surface diffusion of both H and $>C{=}CH_2$ species ($>C$ represents a surface carbon) facilitate incorporation of acetylene into the lattice and that the most efficient way for addition of acetylene to the diamond (100) surface is at biradical sites. Although UHF-MP2 theory is not expected to provide quantitative accuracy for open-shell systems, such predictions are valuable, since once precise growth mechanisms are known, surface modifications (such as the desired type and concentration of defects) can be made to enhance film growth.

In their work, Musgrave et al (76) examined the Garrison-Brenner mechanism (77) for an essential step in diamond (100) film growth, the formation of a six-membered C atom ring from the five-membered C atom ring of which the surface dimer is part. All of the steps except the last one for this process have gas-phase analogs from which rate constants can be estimated. The last step consists of the formation of the six-membered C atom ring from a surface radical ($>CH$) and a surface-olefin ($>C{=}CH_2$), which have formed from surface dimer C atoms (here the $>C$ represents the C atom that was formerly part of the surface dimer). Because of the role of the surface in this process, no gas-phase analogs are available from which to estimate the rate constant. Speculation that the surface-radical-surface-olefin recombination step might be too slow to explain experimentally observed diamond growth led Musgrave et al (76) to

analyze this mechanism. They computed the PES for this final process at the GVB-SDCI level on a small, C_3H_7 cluster for which the surface geometries had been obtained from MP2 calculations on a larger $C_{10}H_{15}$ cluster. The MP2 calculations were also used to estimate the effects of cluster size and to obtain vibrational frequencies for the C_3H_7 cluster from which to estimate the ZPE correction to the barriers and the preexponential in the Arrhenius equation. From their calculations, Musgrave et al (76) predicted that the rate constant for the final surface-radical-surface-olefin recombination step was several orders of magnitude faster than the gas-phase estimates of rate constants for the preceding steps. Thus they concluded, based on these estimates, that diamond film growth can occur via the Garrison-Brenner dimer mechanism.

In the above two studies, large order-of-magnitude differences between rate constants were looked at to determine the importance of specific mechanisms for the growth process. The qualitative nature of these studies is appropriate to the lack of quantitative accuracy available from TST analysis. Nevertheless, the lack of quantitative accuracy should not detract from the valuable insight this method allows into the hierarchy of dynamic processes. Because of the time scale limitations of other types of calculations (e.g. classical MD, QD, and FAIMD), rate constant estimates from TST and simulations of the interplay of these processes using KMC will be important in the quest to fully understand molecule-surface reactions, as we illustrate below.

Fully Ab Initio Molecular Dynamics

There have been exactly three FAIMD treatments of molecule-surface reactions to date. The first FAIMD calculation of a surface reaction was a DFT-BOAIMD calculation of Cl_2 reacting with the Si(111)-2×1 surface (78a–c). In their calculation, Payne and coworkers used DFT-LDA with pseudopotentials (79a,b) for the Cl (80a,b) and Si (81) and $k = 0$ (the Γ point) sampling with a plane-wave cutoff of 136 eV. They used a Si(111)-2×1 surface represented by an eight-layer slab, with each layer having 12 atoms and a $2\sqrt{3} \times 3$ surface unit cell. Unlike classical MD simulations in which it is feasible to obtain many trajectories for different molecular incident energies and angles, for this FAIMD calculation Payne and coworkers used massively parallel computing (82) to report five 200–400 fs trajectories of Cl_2 reacting with the Si(111)-2×1 surface. Because each trajectory was so computationally intensive, they chose to use a translational energy of 1 eV for all simulations, since this would work to ensure that dissociative chemisorption occurred. Furthermore, they strategically chose the initial conditions of each simulation (horizontal and molecular orientation of the Cl_2 in relation to the surface) to investigate specific reaction scenarios. From their limited study, they concluded that Cl_2 incident on Si(111)-2×1 reacts dissociatively, sometimes through a molecular precursor.

While this calculation clearly was state of the art, the lack of *k*-point sampling and of nonlocal corrections to the LDA—both of which are critical to an accurate description of molecular chemisorption with DFT—as well as the obvious lack of good statistics, reminds us that FAIMD is not yet able to provide quantitative predictions for comparison to experiment.

Given this caveat, this type of calculation still provides more insight than other methods (MD, energy difference calculations, and experimentation). Since the wavefunction or density of the system is available for inspection, FAIMD simulations allow examination of which bonds are important to dissociation at every step of the reaction. There is also no bias due to an analytic potential function as to how dissociation depends on the position and orientation of the molecule, how the surface responds to collision/dissociation event, whether there is a precursor state to dissociation after initial collision (i.e. molecular adsorption followed by decomposition), or the amount of momentum transfer between the colliding molecule and surface.

Using this technique to study another technologically relevant reaction, the reaction of F_2 on Si(100)-2 $\times$ 1, would also be an important calculation. However, the second-row element Cl is actually easier to use in DFT calculations, since for first-row elements such as F, soft Vanderbilt pseudopotentials (83a–c) are needed. Making use of such pseudopotentials leads to functional dependence on atomic position that makes the computations much more expensive; terms in the DFT energy and force expressions need to be continually recalculated as the atoms move.

In the second FAIMD study, Langel & Parrinello (84a,b) applied the DFT-based CPAIMD method to molecules on metal oxides. They wanted to discover the site of H_2O dissociation on MgO surfaces. Static energy calculations had predicted that adsorption is unfavorable on a perfect MgO(100) surface, leaving unexplained the experimental observation that H_2O dissociatively chemisorbs on this surface [this conclusion was inferred from infrared studies showing the absence of the H_2O bending vibration for MgO(100) treated with H_2O]. Langel & Parrinello's DFT-CPAIMD used the LDA approach with the GGA described by the Becke (85a,b) exchange functional and $k = 0$ sampling only. To keep their calculation tractable, they used supersoft pseudopotentials of Vanderbilt (83a–c, 86) for O and H and a norm-conserving pseudopotential (87) for Mg. One can consider this an improvement over the study by Payne and coworkers (78a–c), in that some attempt is made for known deficiencies in the LDA. In agreement with static energy calculations, their DFT-AIMD study found that H_2O was only physisorbed. To test the theory that dissociation is mediated at steps, they employed the DFT-AIMD method for H_2O reacting with a stepped MgO surface. The steps were represented by small regions faceting a (110) plane into short (100) terraces that were periodically replicated. Starting with

the H_2O molecules adsorbed on the step, dissociation of the molecules to a H atom adsorbed on a surface O atom and a hydroxyl group adsorbed on a surface Mg atom was complete after ~1 ps. Thus, this study confirmed the idea that steps are crucial to dissociation of H_2O on MgO.

The DFT-AIMD dynamics provided a convenient way of looking at complicated reaction paths occurring on steps and identifying the process through which H_2O dissociation may occur. In these two examples, we have seen that the strong point of these methods is being able to look at complex reaction paths without the need for or bias from an analytic potential. Determining the correct pathway by obtaining the saddle point and endpoints for each possible reaction to dissociation would be a more difficult task. Nonetheless, once the appropriate pathway has been identified, more accurate energy differences could be obtained by using higher level ab initio calculations. Although AIMD studies afford a look into surface reaction dynamics not otherwise available, as mentioned before, they still cannot be counted on to provide a complete picture, owing to the inability to perform enough trajectories to yield adequate statistics. AIMD methods also should not be considered reliable for determining molecular precursor and physisorption states at present, since the energy differences involved in these processes are too small for the accuracy of ab initio methods as typically implemented.

The above two examples of FAIMD use DFT-based methods. The third example of FAIMD applied to molecule-surface reactions is also the first of the WBAIMD type. This simulation is discussed in the following section on H_2-Si(100) reactions.

AIMD Applied to H_2 Desorption and Adsorption on Si(100)

In this section, we look at how different AIMD methods have provided insight into the pathways for adsorption and desorption of H_2 on the Si(100)-2×1 surface. The interaction of hydrogen with silicon surfaces has been well studied by theorists and experimentalists (88) because of the importance of hydrogen as a passivating layer on this surface—hydrogen ties up the reactive dangling bonds on the surface. This can be a desirable effect when surface preservation is the goal; however, film growth using chemical vapor deposition (CVD) can be poisoned by hydrogen in the atmosphere or hydrogen as a by-product of the CVD. Besides the technological importance of H_2 reactions to the semiconductor industry, this reaction possesses intriguing kinetic and dynamic properties. Contrary to intuition, the desorption of H_2 has a kinetic order of one. Chemical intuition based on the desorption reactions of H_2 from Si(111)-7×7 and metals would expect desorption to be the result of two H atoms randomly meeting and recombining on the surface, a process with a kinetic order of two. Another odd feature of H_2 desorption/adsorption on silicon is an apparent violation of

the principle of detailed balance. Application of this principle implies that the adsorption and desorption of H_2 should be through the same pathway. But it is difficult to reconcile this criterion with the experimentally observed low sticking probability of H_2 on silicon and experimental evidence that desorbing H_2 does not come down off of a large barrier to adsorption (i.e. desorbing hydrogen molecules are found, by time-of-flight mass spectrometry, to be not translationally excited) (89a–c).

Because of the technological relevance of this system and the interesting fundamental questions it poses, much theoretical work, including some novel AIMD simulations, has been done on this molecule-surface reaction. Because the first step to describing this reaction is to identify the pathway through which it occurs, this process has been well studied by static ab initio calculations of the barriers for different pathways. However, there has been some disparity between energy barriers calculated with DFT and wavefunction-based quantum mechanics (with agreement between the two methods depending on which functional is used in the DFT calculations), and thus, determining the pathway for desorption/adsorption has not been clear cut. Currently, in some calculations the lowest barrier to desorption is through isolated dihydrides on the Si(100)-2×1 surface, while other calculations support recombinative desorption from H atoms "prepaired" on the same Si surface dimer (the prepairing mechanism) (90).

In our own work on this subject (10a,b), we combined our ab initio PES calculations at the MRSDCI level on embedded clusters (nine to ten Si atoms embedded in H atoms whose basis sets were modified so as not to draw off charge from the Si atoms) with the Hessians we obtained from finite differences of ab initio gradients at the CASSCF level to determine nonvariational STST rate constants. We also corrected the MRSDCI energy barriers with ZPE corrections from the CASSCF level vibrational frequencies. From this analysis we found that although the rate constant for the isolated dihydride mechanism is one to two orders of magnitude below experimental values (which in themselves vary by up to a factor of 16), the rate constants for all mechanisms involving desorption of H atoms on the same surface silicon dimer were at least six orders of magnitude lower. Furthermore, our study of the potential errors involved in our energy barrier calculations suggests an explanation for the too-low rate constant for the isolated dihydride mechanism, but does not modify the six-order-of-magnitude difference between our calculated rate constants for prepairing routes and experiment.

Because internal energy distribution and angular distribution measurements of H_2 desorbing from the Si(100)-2×1 surface are available (88), da Silva et al (91) undertook CASSCF AIMD simulations to test the consistency of the isolated dihydride and prepairing mechanisms with these experimental data. They

used TS geometries determined by our previous work (10a,b) as starting points for WBAIMD trajectories. A sample trajectory for desorption via the dihydride mechanism is shown in Figure 2. The initial velocities for the Si atoms were chosen randomly from a Boltzmann distribution at the peak H_2 desorption temperature. Ten to twenty trajectories at the peak H_2 desorption temperatures were run for desorption via each mechanism. These simulations predicted that desorption through both the isolated dihydride and prepairing mechanisms are consistent with experimental observations that H_2 desorbs rotationally cold, while the isolated dihydride mechanism is in better agreement with the vibrational energy of desorbing H_2. Also, the smaller average angle of the desorbing molecule from the surface normal for H_2 desorbing from the isolated dihydride mechanism versus the prepairing mechanism agrees with the relatively focused angular distributions of D_2 desorption from Si(100)-2 $\times$ 1 (92).

Two recent QD simulations (93, 94) using DFT-derived potentials were performed to investigate how the prepairing mechanism might be reconciled with the apparent violation of detailed balance of this reaction and also with recent experiments that show that the sticking probability of H_2 increases with rising temperature (89a–c, 95). DFT and our MRSDCI calculations predict a low sticking probability for adsorption through the prepairing mechanism based on the high barrier to adsorption calculated. This prediction agrees with the experimentally observed low sticking probability but not with experimental observations that H_2 desorbs translationally cold, presumably a result of not coming down off of a high barrier (89a–c). [In another paper (10a,b), we give a detailed analysis of how orientational constraints and defect concentration could make adsorption and desorption through the isolated dihydride mechanism consistent with experimental observations.]

To test the idea that the H_2 may desorb translationally cold via the prepairing mechanism because the excess energy might be transferred into surface phonons, Luntz & Kratzer (93) performed QD and quasiclassical simulations of D_2 interacting with Si(100)-2 $\times$ 1 by using a PES that consisted of three degrees of freedom: the distance of the D_2 center-of-mass to the surface, the D-D bond length, and a surface Si phonon coordinate. They used wavepacket QD on the three-dimensional, DFT-derived PES to determine the temperature dependence of the sticking probability. To test the idea that energy transfer into lattice vibrations during desorption could make desorption through the prepairing mechanism consistent with experimental measurements of product state distributions, they used a three-dimensional quasiclassical approach employing the same DFT-derived PES. Luntz & Kratzer (93) deemed the quasiclassical approach suitable for modeling desorption, since their initial two-dimensional QD calculations indicated that tunneling did not have a considerable influence

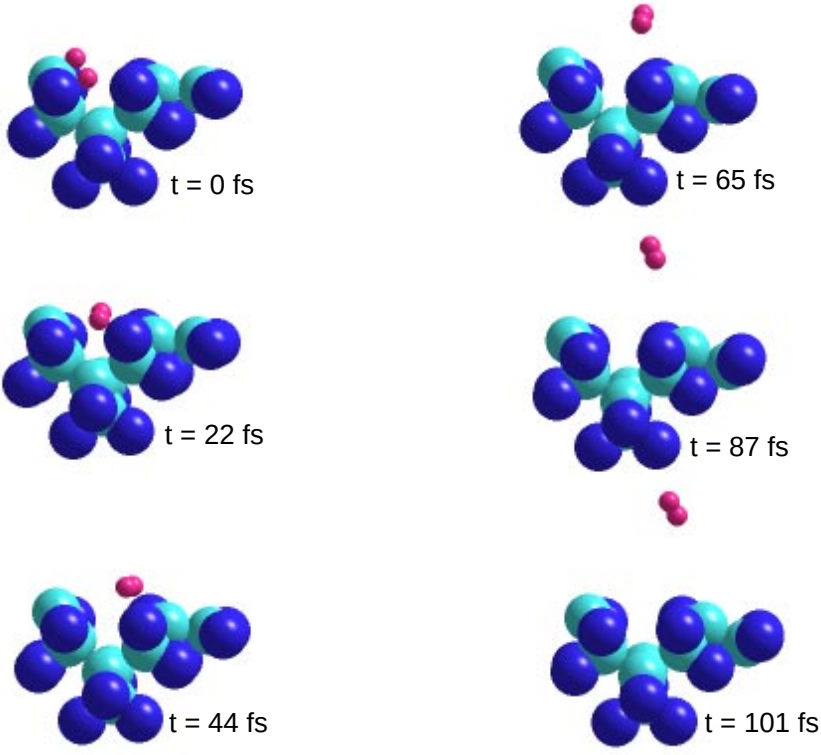

Figure 2 Snapshots from a fully ab initio MD simulation of H_2 desorbing from Si(100), starting from the transition state for desorption via a dihydride desorption precursor. The H atoms are the small spheres, the larger light gray spheres are silicon atoms, and the larger dark gray spheres are embedding atoms. Note that while the structure of the transition state ($t = 0$) would suggest a very broad angular distribution, the corrugated nature of the surface allows the H_2 to scatter off of a neighboring dimer and become refocused more toward the surface normal. (From Reference 91.) [A color version of this figure is available on the World Wide Web in the Supplementary Materials Section of the main Annual Reviews Inc. site (http://www.annurev.org).]

on this desorption process. The results of both simulations demonstrate that desorption and adsorption through the prepairing mechanism are not consistent with experimental evidence, as adsorption was found to have only a weak dependence on temperature, and there was insufficient energy transfer to the substrate lattice during the desorption process. The authors discussed several reasons for the disagreement of their model with experiment, including shortcomings in the method and, possibly, the lack of importance of the prepairing mechanism in the real system.

A similar three-dimensional QD calculation for H_2 adsorption/desorption from Si(100)-2 $\times$ 1 was undertaken by Kratzer et al (94) to test the same theory. They found a larger temperature dependence of the sticking probability on temperature than reported by Luntz & Kratzer (93). In their work, Luntz & Kratzer attributed the difference in the results of these two simulations to different models of the PES. They suspected that the PES used by Kratzer et al (94) neglected effects evident from existing ab initio data. A higher-dimensional model is apparently necessary in order to properly quantify the role of the substrate in the desorption process. This type of information may not be available from the cluster calculation of da Silva et al (91): Although more degrees of freedom were included in this calculation, the finite nature of the cluster may preclude the occurrence of realistic energy transfer.

The prepairing mechanism was originally proposed because the prepairing of H atoms prior to desorption provided an explanation for the first-order kinetics of H_2 desorption from Si(100)-2 $\times$ 1. To see if the isolated dihydride mechanism also could explain the first-order kinetics, we looked at the desorption process using a KMC simulation with a hierarchy of rates determined from experimental and ab initio MRSDCI data (96). The type of processes included in the model were H and Si atom diffusion, various hydride isomerizations, and H_2 desorption. This model was able to show the effects of coverage, temperature, and defect concentration on desorption kinetics. Because of the long time scale of desorption events relative to other surface processes that potentially lead to desorption and to keep the simulation tractable, a one-dimensional array of surface dimers and defects was used to model the surface with the fast step of diffusion along dimer rows incorporated in a random mixing process. (The one-dimensional model is sufficient, since all of the steps important for desorption actually do occur along a chain of dimers.) From our KMC model, we found that the kinetics for H_2 desorption via the isolated dihydride mechanism are first order regardless of surface coverage, temperature, or defect concentration. We also found that the rate constant increased significantly with increasing defect concentration, which provided an explanation for the range of values observed in different laboratories. We emphasize that these KMC calculations

were critical to proving that our isolated dihydride mechanism also yields the unusual first-order dependence on hydrogen coverage observed experimentally.

The dynamic calculations above look at different aspects of the H_2–Si(100)-2×1 adsorption/desorption reaction. These models both test specific mechanisms for experimental compatibility and predict behavior that should occur as a result of these mechanisms, thus driving further experimental studies.

Accuracy Issues for Ab Initio Calculations

Thus far we have concentrated on AIMD methods and their applications. However, AIMD methods are intertwined with the reliability of the ab initio calculations they use whether these calculations are determining energetics for fitting a potential, estimating rate constants, or are used on the fly in FAIMD. Therefore, we feel that it is important to address the accuracy of these calculations as a separate issue.

From previous studies (97–100), it is apparent that the least computationally intensive form of DFT, the LDA, is also the least reliable for predicting adsorption barriers. These studies considered H_2 dissociating on Al(110) (97), Cu(100) (98), and Cu(111) (99), and CO chemisorption on Pd(110) (100). The general conclusion from these investigations was that the LDA significantly underestimates dissociation barriers and overestimates chemisorption energies, while gradient-corrected DFT (GGA) calculations often predict energies closer to experimental results. On the other hand, work by Kaxiras and coworkers (101a,b) looked at how well several gradient-corrected functionals predicted known metal and semiconductor bulk properties. They found that while the GGA gives results closer to experiment for cohesive energies than the LDA, the GGA functionals they examined gave nonsystematic changes in properties. Similar conclusions had been reached earlier by Louie, Cohen, and coworkers (102). It is indeed unclear from a purely theoretical point of view if we will ever achieve converged and systematic predictions using gradient corrections, as it is clear that for the exact ground state densities of finite systems, the gradient expansion diverges (103).

Jordan and coworkers (104) attempted to determine which DFT functionals produced results closest to experiment for the H_2-Si(100) adsorption/desorption puzzle discussed above. We mentioned above that energetics computed using different ab initio methods predicted different pathways for desorption. Specifically, DFT using the Becke3LYP functional (14) and MRSDCI (10a,b, 15) methods predict that the barrier for desorption via the prepairing mechanism is too high, while other DFT calculations using different functionals and kinetic energy cutoffs in the plane-wave basis expansion predict a range of barriers, some of which agree well with experimental values (105a–109). Jordan and

coworkers (104) used different quality functionals to examine reactions of small gas-phase silanes (Si_xH_y), reactions for which the pathway and the energetics were well known experimentally. Since H_2 elimination from disilane Si_2H_4 and from silane (SiH_4) are analogous reactions to hydrogen desorbing from a silicon dimer and an isolated silicon surface atom, respectively, Jordan and coworkers reasoned that their study would provide insight into the error in ab initio calculations of the energetics of these surface reactions. Indeed, TSs found by us (10a,b) at the CASSCF level of theory predict that these gas-phase reaction TSs closely resemble their surface reaction counterparts.

What Jordan and coworkers (104) found was that less accurate functionals significantly underestimated the activation barriers for these gas-phase reactions, while the better quality Becke3LYP functional yields predictions that are closer to experiment. When Jordan and coworkers (14) used the more accurate Becke3LYP functional in cluster calculations of the H_2 desorption activation energy, their predicted value matched those obtained with MRSDCI methods. This study provides systematic evidence that using inferior functionals leads to the underestimation of activation barriers and suggests the need to further benchmark DFT functionals against known activation barriers. Thus, from the investigations discussed above, we conclude that state-of-the-art DFT-AIMD should consist of nonlocal DFT with better quality functionals.

Outlook and Conclusions

In this review we have attempted to give the reader a flavor for what current AIMD methods consist of, what can and cannot be accomplished using these techniques, and what comprises practical, computationally feasible simulations. The most compelling demands on AIMD at the present are the need for better scaling methods to enable theorists to study larger systems on longer time scales. Toward this horizon, there has been progress in linear scaling DFT-MD (110a–e) and (ab initio–derived) tight-binding MD (110e, 111a,b) methods. We also feel that hybrid methods such as DFT or tight binding for long length scale and ab initio CI calculations for localized interactions hold promise (112).

DFT methods are currently the fastest ab initio techniques for energy and gradient calculations, but there is a profound need for systematic improvement in treatment of electron correlation in DFT before this theory can be relied upon to yield accurate energy differences and dynamics. On the other hand, advances or hybridizations with other methods must be made before WBAIMD methods become applicable to a wide range of surface processes, particularly for reactions occurring on metals. With improved theories, AIMD will begin playing an important role in surface chemistry.

ACKNOWLEDGMENTS

We would like to thank Dr. Antonio da Silva and Dr. Paul C Weakliem for graciously preparing the figures. EAC acknowledges support from the Air Force Office of Scientific Research, the Office of Naval Research, the National Science Foundation, the Army Research Office, the Camille and Henry Dreyfus Foundation, the Alfred P. Sloan Foundation, Olin Chemical Corporation, Rohm & Haas, and Union Carbide during the course of the research associated with this topic.

Literature Cited

1. Whitten JL, Yang H. 1996. *Surf. Sci. Rep.* 24:59–124
2a. Kosloff R. 1996. In *Dynamics of Molecular and Chemical Reactions,* ed. J Zhang, RE Wyatt, pp. 185–230. New York: Marcel Dekker
2b. Kosloff R. 1994. *Annu. Rev. Phys. Chem.* 45:145–78
3a. Gross A, Wilke S, Scheffler M. 1995. *Phys. Rev. Lett.* 75:2718–21
3b. Gross A, Wilke S, Scheffler M. 1996. *Surf. Sci.* 358:614–18
3c. Gross A. 1996. *Surf. Sci.* 363:1–10
4. Allen MP, Tildesley DJ. 1987. *Computer Simulation of Liquids.* New York: Oxford Univ. Press
5. Fichthorn KA, Weinberg WH. 1991. *J. Chem. Phys.* 95:1090–96
6a. Doll JD. 1980. *J. Chem. Phys.* 73:2760–62
6b. Doll JD. 1981. *J. Chem. Phys.* 74:1074–77
6c. Voter AF, Doll JD. 1985. *J. Chem. Phys.* 82:80–92
6d. Voter AF, Doll JD. 1984. *J. Chem. Phys.* 80:5814–17
6e. Voter AF, Doll JD. 1984. *J. Chem. Phys.* 80:5832–38
6f. Voter AF. 1986. *Phys. Rev. B* 34:6819–29
7. NoorBatcha I, Raff LM, Thompson DL. 1985. *J. Chem. Phys.* 83:1382–91
8. Truhlar DG, Hase WL, Hynes JT. 1983. *J. Phys. Chem.* 87:2664–82
9. Steinfeld JI, Francisco JS, Hase WL. 1989. *Chemical Kinetics and Dynamics.* Englewood Cliffs, NJ: Prentice Hall
10a. Radeke MR, Carter EA. 1996. *Surf. Sci. Lett.* 355:L289–94
10b. Radeke MR, Carter EA. 1996. *Phys. Rev. B* 54:11803–17
11a. Wu CJ, Carter EA. 1991. *Chem. Phys. Lett.* 185:172–78
11b. Wu CJ, Carter EA. 1991. *J. Am. Chem. Soc.* 113:9061–62
11c. Wu CJ, Carter EA. 1992. *Phys. Rev. B* 46:4651–58
11d. Wu CJ, Ionova IV, Carter EA. 1993. *Surf. Sci.* 295:64–78
12. Wu CJ, Carter EA. 1992. *Phys. Rev. B* 45:9065–81
13. Redondo A, Goddard WA III. 1982. *J. Vac. Sci. Technol.* 21:344–50
14. Nachtigall P, Jordan KD, Sosa C. 1994. *J. Chem. Phys.* 101:8073–81
15. Jing Z, Whitten JL. 1995. *J. Chem. Phys.* 102:3867–72
16a. Hohenberg P, Kohn W. 1964. *Phys. Rev. B* 136:864–71
16b. Jones RO, Gunnarsson O. 1989. *Rev. Mod. Phys.* 61:689–746
17. Car R, Parrinello M. 1985. *Phys. Rev. Lett.* 55:2471–74
18. Kohn W, Sham LJ. 1965. *Phys. Rev. A* 140:1133–38
19a. Barnett RN, Landman U, Nitzan A, Rajagopal G. 1991. *J. Chem. Phys.* 94:608–16
19b. Wentzcovitch RM, Martins JL. 1991. *Solid State Commun.* 78:831–34
20. Payne MC, Teter MP, Allan DC, Arias TA, Joannopoulos JD. 1992. *Rev. Mod. Phys.* 64:1045–97
21a. Bachelet GB, Hamann DR, Schluter M. 1982. *Phys. Rev. B* 26:4199–228
21b. Pickett WE. 1989. *Comp. Phys. Rep.* 9:115–97

22. Hartke B, Carter EA. 1992. *Chem. Phys. Lett.* 189:358–62
23. Field MJ. 1991. *J. Phys. Chem.* 95:5104–8
24. Hartke B, Carter EA. 1992. *J. Chem. Phys.* 97:6569–78
25. Bobrowicz FW, Goddard WA III. 1977. *Methods of Electronic Structure Theory,* 3:79–127. New York: Plenum
26. Liu Z, Carter LE, Carter EA. 1995. *J. Phys. Chem.* 99:4355–59
27. Roos BO. 1987. *Adv. Chem. Phys.* 69:399
28. Siegbahn PEM. 1980. *J. Chem. Phys.* 74:1647
29. Gibson DA, Ionova IV, Carter EA. 1995. *Chem. Phys. Lett.* 240:261–67
30. da Silva AJR, Gibson DA, Carter EA. 1996. Unpublished data
31a. Weakliem PC, Wu CJ, Carter EA. 1992. *Phys. Rev. Lett.* 69:200–3
31b. Weakliem PC, Carter EA. 1993. *J. Chem. Phys.* 98:737–45
32. Stillinger FH, Weber TA. 1989. *Phys. Rev. Lett.* 62:2144–47
33. Weber TA, Stillinger FH. 1990. *J. Chem. Phys.* 92:6239–45
34. Li YL, Pullman DP, Yang JJ, Tsekouras AA, Gosalvez DG, et al. 1995. *Phys. Rev. Lett.* 74:2603–6
35. Schoolcraft TA, Garrison BJ. 1991. *J. Am. Chem. Soc.* 113:8221–28
36a. Wu CJ, Carter EA. 1991. *J. Am. Chem. Soc.* 113:9061–62
36b. Wu CJ, Carter EA. 1992. *Phys. Rev. B* 45:9065–81
37. Lo CW, Varekamp PR, Shuh DK, Yarmoff JA. 1993. *Surf. Sci.* 292:171–81
38. Carter LE, Carter EA. 1996. *Surf. Sci.* 360:200–12
39. Carter LE, Carter EA. 1996. *J. Phys. Chem.* 100:873–87
40a. Carter LE, Khodabandeh S, Weakliem PC, Carter EA. 1994. *J. Chem. Phys.* 100:2277–88
40b. Carter LE, Carter EA. 1994. *J. Vac. Sci. Technol. A* 12:2235–39
40c. Carter LE, Carter EA. 1995. *Surf. Sci.* 323:39–50
41. Jensen JA, Yan C, Kummel AC. 1995. *Science* 267:493–96
42. Schoolcraft TA, Diehl AM, Steel AB, Garrison BJ. 1995. *J. Vac. Sci. Technol. A* 13:1861–66
43. Kara A, DePristo AE. 1990. *J. Chem. Phys.* 92:5653–60
44. Lee CY, DePristo AE. 1986. *J. Chem. Phys.* 85:4161–71
45a. Panas I, Siegbahn P, Wahlgren U. 1988. *Theor. Chim. Acta* 74:167–89
45b. Siegbahn P, Blomberg M, Panas I, Wahlgren U. 1989. *Theor. Chim. Acta* 75:143–59
46. Hamza AV, Madix RJ. 1985. *J. Phys. Chem.* 89:5381–86
47. Michelsen HA, Rettner CT, Auerbach DJ. 1994. In *Surface Reactions,* ed. RJ Madix, *Springer Ser. Surf. Sci.* 34:185–237. Berlin: Springer-Verlag
48. Jackson B, Metiu H. 1987. *J. Chem. Phys.* 86:1026–35
49. Bourcet A, Tantardini GF. 1994. *J. Electron Spectrosc. Relat. Phenom.* 69:55–64
50. Forni A, Tantardini GF. 1996. *Surf. Sci.* 352–54:142–147
51a. Yang H, Whitten JL. 1988. *J. Chem. Phys.* 89:5329–34
51b. Yang H, Whitten JL. 1991. *Surf. Sci.* 255:193–207
52. Yang H, Whitten JL. 1993. *J. Chem. Phys.* 98:5039–49
53. Holloway S, Darling GR. 1995. *Appl. Phys. A* 61:511–17
54. Holloway S. 1994. *Surf. Sci.* 299/300:656–66
55. Darling GR, Holloway S. 1995. *Rep. Prog. Phys.* 58:1595–672
56. Bird DM, Clarke LJ, Payne MC, Stich I. 1993. *Chem. Phys. Lett.* 212:518–24
57a. Hammer B, Scheffler M, Jacobsen KW, Nørskov JK. 1994. *Phys. Rev. Lett.* 73:1400–3
57b. White JA, Bird DM, Payne MC, Stich I. 1994. *Phys. Rev. Lett.* 73:1404–7
58. Siegbahn PEM, Blomberg MRA, Bauschlicher CW Jr. 1984. *J. Chem. Phys.* 81:2103–11
59. Gundersen K, Jacobsen KW, Nørskov JK, Hammer B. 1994. *Surf. Sci.* 304:131–44
60. Perdew JP, Zunger A. 1981. *Phys. Rev. B* 23:5048–79
61. White JA, Bird DM. 1994. *Phys. Rev. B* 50:4954–57
62. Kinnersley AD, Darling GR, Holloway S, Hammer B. 1996. *Surf. Sci.* 364:219–34
63a. Wilke S, Scheffler M. 1995. *Surf. Sci.* 329:L605–10
63b. Wilke S, Scheffler M. 1996. *Phys. Rev. B* 53:4926–32
64. Gross A, Wilke S, Scheffler M. 1995. *Phys. Rev. Lett.* 75:2718–21
65. Gross A. 1996. *Surf. Sci.* 363:1–10
66. Gross A, Hammer B, Scheffler M, Brenig W. 1994. *Phys. Rev. Lett.* 73:3121–24
67. Kay M, Darling GR, Holloway S, White JA, Bird DM. 1995. *Chem. Phys. Lett.* 245:311–18

68. Darling GR, Holloway S. 1992. *J. Chem. Phys.* 97:734–36
69. Saalfrank P, Holloway S, Darling GR. 1995. *J. Chem. Phys.* 103:6720–34
70. Møller C, Plesset MS. 1934. *Phys. Rev.* 46:618
71. Szabo A, Ostlund NS. 1989. *Modern Quantum Chemistry.* New York: McGraw-Hill
72. Huzinaga S. 1985. In *Physical Science Data: Gaussian Basis Sets for Molecular Calculations*, Vol. 16, ed. S Huzinaga. New York: Elsevier
73. Hermann K, Bagus PS. 1979. *Phys. Rev. B* 20:20
74. Raff LM, NoorBatcha I, Thompson DL. 1986. *J. Chem. Phys.* 85:3081–89
75. Skokov S, Weiner B, Frenklach M. 1995. *J. Phys. Chem.* 99:5616–25
76. Musgrave CB, Harris SJ, Goddard WA III. 1995. *Chem. Phys. Lett.* 247:359–65
77. Johnson CE, Weimer WA, Cerio FM. 1992. *J. Mater. Res.* 7:1427–31

78a. De Vita A, Stich I, Gillan MJ, Payne MC, Clarke LJ. 1993. *Phys. Rev. Lett.* 71:1276–79

78b. Stich I, De Vita A, Payne MC, Gillan MJ, Clarke LJ. 1994. *Phys. Rev. B* 49:8076–85

78c. Stich I, Payne MC, De Vita A, Gillan MJ, Clarke LJ. 1993. *Chem. Phys. Lett.* 212:617–23

79a. Kleinman L, Bylander DM. 1980. *Phys. Rev. Lett.* 48:1425

79b. King-Smith RD, Payne MC, Lin J-S. 1991. *Phys. Rev. B* 44:13063–66

80a. Rappe A, Rabe KM, Kaxiras E, Joannopoulos JD. 1990. *Phys. Rev. B* 41:1227–30

80b. Lin J-S, Qteish A, Payne MC, Heine V. 1993. *Phys. Rev. B* 47:4174–80

81. Kerker GP. 1980. *J. Phys. C* 13:L189
82. Clarke LJ, Stich I, Payne MC. 1992. *Comput. Phys. Commun.* 72:14–28

83a. Vanderbilt D. 1990. *Phys. Rev. B* 41: 7892–95

83b. Laasonen K, Car R, Lee C, Vanderbilt D. 1991. *Phys. Rev. B* 43:6796–99

83c. Laasonen K, Pasquarello A, Car R, Lee C, Vanderbilt D. 1993. *Phys. Rev. B* 47:10142–53

84a. Langel W, Parrinello M. 1994. *Phys. Rev. Lett.* 73:504–7

84b. Langel W, Parrinello M. 1995. *J. Chem. Phys.* 103: 3240–52

85a. Becke AD. 1988. *Phys. Rev. A* 38:3098–100

85b. Becke AD. 1992. *J. Chem. Phys.* 96: 2155–60

86. Laasonen K, Sprik M, Parrinello M, Car R. 1993. *J. Chem. Phys.* 99:9080–89
87. Stumpf R, Gonze X, Scheffler M. 1990. *Res. Rep. Fritz-Haber Inst.*
88. Kolasinski KW. 1995. *Int. J. Mod. Phys. B* 9:2753–809

89a. Kolasinski KW, Nessler W, de Meijere A, Hasselbrink E. 1994. *Phys. Rev. Lett.* 72:1356–59

89b. Kolasinski KW, Nessler W, Bornscheuer K-H, Hasselbrink E. 1995. *Surf. Sci.* 331:485–89

89c. Kolasinski KW, Nessler W, Bornscheuer K-H, Hasselbrink E. 1994. *J. Chem. Phys.* 101:7082–94

90. Radeke MR, Carter EA. 1996. *Phys. Rev. B* 54:11803–17
91. da Silva AJR, Radeke MR, Carter EA. 1997. *Surf. Sci. Lett.* 381:628–35
92. Park Y-S, Bang J-S, Lee J. 1993. *Surf. Sci.* 283:209–12
93. Luntz AC, Kratzer P. 1996. *J. Chem. Phys.* 104:3075–91
94. Kratzer P, Russ R, Brenig W. 1996. *Surf. Sci.* 345:125–37
95. Bratu P, Kompa KL, Höfer U. 1996. *Chem. Phys. Lett.* 251:1–7
96. Radeke MR, Carter EA. 1997. *Phys. Rev. B* 55:4649–58
97. Hammer B, Jacobsen KW, Nørskov JK. 1993. *Phys. Rev. Lett.* 70:3971–74
98. White JA, Bird DM, Payne MC, Stich I. 1994. *Phys. Rev. Lett.* 73:1404–7
99. Hammer B, Scheffler M, Jacobsen KW, Nørskov JK. 1994. *Phys. Rev. Lett.* 73:1400–3
100. Hu P, King DA, Crampin S, Lee M-H, Payne MC. 1994. *Chem. Phys. Lett.* 230:501–6

101a. Juan Y-M, Kaxiras E. 1993. *Phys. Rev. B* 48:14944–52

101b. Juan Y-M, Kaxiras E, Gordon RG. 1995. *Phys. Rev. B* 51:9521–25

102. Garcia A, Elsasser C, Zhu J, Louie SG, Cohen ML. 1992. *Phys. Rev. B* 46:9829–32
103. Dreizler RM, Gross EKU. 1990. *Density Functional Theory—An Approach to the Quantum Many-Body Problem*, p. 95. Berlin: Springer-Verlag
104. Nachtigall P, Jordan KD, Smith A, Jónsson H. 1996. *J. Phys. Chem.* 104: 148–58

105a. Kratzer P, Hammer B, Nørskov JK. 1994. *Chem. Phys. Lett.* 229:645–49

105b. Kratzer P, Hammer B, Nørskov JK. 1995. *Phys. Rev. B* 51:13432–40

106. Pehlke E, Scheffler M. 1995. *Phys. Rev. Lett.* 74:952–55
107. Pai S, Doren D. 1995. *J. Chem. Phys.* 103:1232–34

108. Vittadini A, Selloni A. 1995. *Chem. Phys. Lett.* 235:334–40
109. Li G, Chang Y-C, Tsu R, Greene JE. 1995. *Surf. Sci.* 330:20–26
110a. Pearson M, Smargiassi E, Madden PA. 1993. *J. Phys. Condens. Matter* 5:3221–40
110b. Smargiassi E, Madden PA. 1994. *Phys. Rev. B* 49:5220–26
110c. Foley M, Madden PA. 1996. *Phys. Rev. B* 53:10589–98
110d. Mauri F, Galli G, Car R. 1993. *Phys. Rev. B* 47:9973–76
110e. Mauri F, Galli G. 1994. *Phys. Rev. B* 50:4316–26
111a. Wilson JH, Todd JD, Sutton AP. 1990. *J. Phys. Condens. Matter* 2:10259–88
111b. Ordejon P, Drabold DA, Grumbach MP, Martin RM. 1993. *Phys. Rev. B* 48:14646–49
112. Govind N, da Silva AJR, Carter EA. 1997. Unpublished data